Neurochemical Research (2020) 45:2499–2515
https://doi.org/10.1007/s11064-020-03108-w

ORIGINAL PAPER

Luteolin Protects Against CIRI, Potentially via Regulation of the SIRT3/AMPK/mTOR Signaling Pathway

Shuwen Liu[1,2] · Yu Su[1] · Bixi Sun[1] · Rubin Hao[1,2] · Siqi Pan[1] · Xiaoshu Gao[1] · Xinyue Dong[1] · Ahmed Mohammed Ismail[1] · Bing Han[1]

Received: 3 November 2019 / Revised: 28 June 2020 / Accepted: 1 August 2020 / Published online: 18 August 2020

Abstract

Mitochondrial abnormalities accelerate the progression of ischemic brain damage. Sirtuin 3 (SIRT3) is mainly found in mitochondria and affects almost all major aspects of mitochondrial function. Luteolin, a flavonoid with diverse biological properties, including antioxidant activity, inhibition of cell apoptosis and regulation of autophagy. It also modulates the activity of AMP activated kinase and/or sirtuin 1 (SIRT 1) by regulating the expression of sirtuins. We investigated the protective effects of luteolin on cerebral ischemia-reperfusion. It was found through experiments that luteolin reduced the infarcted area of MCAO rat model, and based on the experimental results, it was inferred that luteolin affected the AMPK, mTOR and SIRT3 pathways, thereby protecting brain cells. As expected, we found that luteolin can reduce the neurological function score, the degree of cerebral edema, the cerebral infarction volume, alleviate morphological changes in the cortex and hippocampus, increase neuron survival and decrease the number of apoptotic neurons. At the same time, luteolin significantly reduced the number of GFAP and Iba-1 positive glial cells in the hippocampus while enhanced the scavenging of oxygen free radicals and the activity of SOD in mitochondria. Addtionally, it can also enhance antioxidant capacity via the reversal of mitochondrial swelling and the mitochondrial transmembrane potential. Moreover, luteolin can increase SIRT3-targeted expression in mitochondria, decrease the phosphorylation of AMPK, and increase phosphor-mTOR (p-mTOR) levels, which may have occurred specifically through activation of the SIRT3/AMPK/mTOR pathway. We speculate that luteolin reduces the pathological progression of CIRI by increasing SIRT3 expression and enhancing mitochondrial function. Therefore, the results indicate that luteolin can increase the transduction of SIRT3, providing a potential mechanism for neuroprotective effects in patients with cerebral ischemia.

Keywords Luteolin · Cerebral ischemia-reperfusion injury · Neuroinflammation · Oxidative stress · Cell apoptosis · SIRT3/AMPK/mTOR signaling pathway

Introduction

Modern research has shown that the pathogenesis of cerebral ischemia-reperfusion injury (CIRI) is caused by multiple factors. Its pathogenesis involves cell failure caused by energy metabolism, excitatory amino acid toxicity, free radical damage, calcium overload, nerve cell apoptosis and inflammatory molecule release [1, 2]. However, the exact molecular mechanism underlying ischemic neuronal injury has not been fully elucidated.

Mitochondria are the "engine" of cells and the key organelles involved in intracellular energy production, and they are known as the "power plant" of the cell [3]. Mitochondrial dysfunction may lead to ROS production and irreversible damage to proteins, lipids and DNA structures [4]. At the same time, the mitochondrial oxidative stress process causes severe destruction of the cytoskeleton, interferes with cell energy metabolism, and participates in a series of pathophysiological processes that include microcirculatory disorders, vascular endothelial cell damage and blood-brain barrier destruction. Neurons are particularly sensitive to mitochondrial dysfunction, and increased ROS

✉ Bing Han
Hanb@jlu.edu.cn

[1] Department of Biopharmacy, School of Pharmaceutical Sciences, Jilin University, Changchun 130021, People's Republic of China

[2] Institute of Traditional Chinese Medicine, Changchun University of Chinese Medicine, Jilin, China

concentration promotes cell death and protein deposition and thus accelerates the apoptosis of neurons in brain tissue. Therefore, mitochondrial dysfunction is considered to be one of the hallmarks of neuronal death induced by CIRI. Maintaining mitochondrial function is key to promoting neuronal survival and neurological function [5].

SIRT3 is a nicotinamide adenine dinucleotide-dependent histone/nonhistone deacetylase [6]. It is the basic deacetylase in mitochondria, and 65% of mitochondrial proteins contain acetyllysine, suggesting that SIRT3 plays an important role in molecular modification [7]. SIRT3 can maintain the intracellular homeostasis balance and plays a crucial part in mitochondrial oxidative metabolism, energy metabolism, signal regulation and apoptosis. Its abnormal function can cause mitochondrial metabolic disorders, cell damage, and even lead to apoptosis [8]. In addition, SIRT3 repairs or clears damaged mitochondria by regulating mitochondrial dynamics and mitochondrial autophagy, thus maintaining the stability and quality of mitochondria [9]. When cells are under stress, the long-chain form of SIRT3 is processed by the matrix, and the peptidase MPP hydrolyzes the N-terminal mitochondrial targeting sequence, which generates the enzyme-catalyzed short-chain form of SIRT3 that can enter the mitochondria to perform its function [10].

Recently, it was found that knockout of the SIRT3 gene significantly inhibited AMPK activation mediated by a grape-derived antioxidant [11]. This was due to the fact that SIRT3 can deacetylate and activate LKB1 (liver kinase B1), and active LKB1 can phosphorylate AMPK to activate AMPK [12]. SIRT3 can act as a "bridge" between AMPK and LKB1 and increase the phosphorylation of AMPK-Thr172 by promoting binding between AMPK and LKB1 [13, 14]. AMPK mainly regulates catabolism, while mTOR mainly affects biosynthesis, both of which play an important role in regulating the balance of cell metabolism. In addition, AMPK is an important regulatory factor for autophagy and plays a positive role in autophagy by acting on the mTOR and ULK1 complexes. These findings suggest that SIRT3 is a regulatory factor of mitochondrial autophagy. It has been suggested that the key function of SIRT3 is to regulate the activity of the AMPK/mTOR signaling pathway and that increased SIRT3 can activate AMPK [15]. Moreover, SIRT3 can regulate the activity of AMPK and mTOR by inducing the expression of the AMPK regulatory subunit [16]. These results suggested that SIRT3 may be involved in the regulation of AMPK and the mTOR signaling pathway.

The flavonoid luteolin (3′,4′,5,7-tetrahydroxyflavone; Fig. 1a) is abundant in pepper, celery, broccoli, thyme, and chamomile tea and has been shown to enter the brain, where it has significant neuroprotective effect [17]. It has been proven that luteolin can reduce oxidative stress, has anti-inflammatory and antiallergy effects, and can inhibit apoptosis and reduce neuronal damage [18, 19]. It can regulate

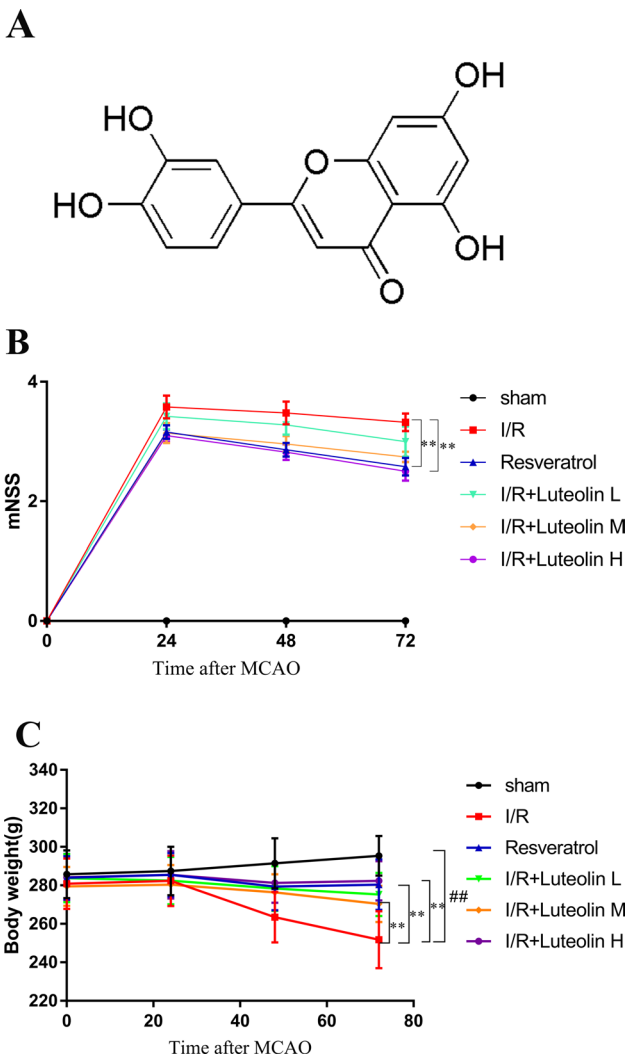

Fig. 1 The neuroprotective effects of luteolin on cerebral I/R in rats. **a** The basic structure of luteolin. **b** A five-point scoring system was used to evaluate neurological deficits after reperfusion. **c** Changes in body weight in rats after reperfusion. The results are expressed as the mean ± standard deviation (SD). $^{\#\#}P < 0.01$, I/R vs the sham group; $^{**}P < 0.01$, vs the I/R group.

mitochondrial function and promote autophagy and has significant neuroprotective effects in Alzheimer's disease, cerebral ischemia injury, epilepsy and Parkinson's disease [20–23]. This study was first to demonstrate that luteolin has an effect on the expression of SIRT3 after CIRI and has neuroprotective effects. Although other studies have shown that SIRT3 has neuroprotective effects in Alzheimer's disease and ischemic cell models as well as oxidative stress neuronal models, most of them have focused on changes in SIRT3 after CIRI, and the role of drugs in increasing the expression of SIRT3 and their effects on mitochondrial protection mechanisms are not completely clear. Therefore, it is significant to investigate the expression of luteolin-activated SIRT3 and its effects on the downstream AMPK/

mTOR pathway in inhibiting neuritis, apoptosis and oxidative stress and promoting nerve regeneration after CIRI. This investigation may provide a new strategy for the treatment of cerebral ischemia-reperfusion injury.

Materials and Methods

Drug

Luteolin with a purity of > 98% was purchased from Sigma-Aldrich Co. (St. Louis, MO, USA). The luteolin was dissolved in sodium hydrogen carbonate and adjusted to a pH value of 7.0, and the final concentration of the luteolin solution was 3.75 mg/ml. After the CIRI model was generated, the rats were subjected to luteolin intraperitoneal injection (15, 30, or 60 mg/kg) for 3 days. The activator (50 mg/kg resveratrol) was dissolved in normal saline and then administered via gavage.

Animals

Eighteen-month-old adult Male and female Sprague-Dawley rats (weighing 250-300 g) were purchased from the animal center of Liaoning Changsheng biotechnology co., Ltd. (certificate number: SCXK, (Liao) 2015-0001). The temperature of the feeding environment was controlled at 21 ± 1 °C, the relative humidity was 60 ± 10%, and the day/night cycle was maintained at 12 h/12 h. The rats had free access to a standard rodent pelleted diet and water ad libitum. All procedures conformed to the guidelines of the Ethics Committee of Jilin University. All animals were acclimatized for at least 1 week prior to the treatments.

Rat Model of Focal Cerebral Ischemia

Based on the method used by Longa et al, an animal model of focal cerebral ischemia was established. A solution of 10% chloral hydrate was intraperitoneally injected into the rats (350 $mg \cdot kg^{-1}$). The rats were supine, fixed, and the skin was cut on the front of the neck. The common carotid artery (CCA) and vagus nerve were separated, and the CCA was threaded alternately; the intracranial (ICA) and extracranial (ECA) arteries were directly separated and threaded for use. The upper thyroid artery and the occipital artery separated by the ECA were burned with a coagulator; the ECA proximal and distal ends were ligated, and the ECA was cut in the middle. The pterygopalatine artery (PA) was ligated, and the thin threads in the CCA and the ICA were tightened to block the blood flow; a small opening was cut in the ECA near the CCA bifurcation, and the plug was threaded through the small opening in the ICA and slowly advanced forward until resistance was encountered. The insertion depth of the thread plug was approximately (18.0 ± 0.5) mm. After the plug was successfully inserted, the thread plug end was left at approximately 1 cm, and the ligature in the ECA was cut and the thin thread in the CCA was loosened. It was noted whether there was bleeding, and the thin thread plug in the CCA and the ICA were removed; the skin was sutured and penicillin sodium solution was injected into the incision to prevent infection. Attention was given intraoperatively and postoperatively to animal warmth and the maintenance of anal temperature (37.0 ± 0.5 °C) and room temperature (26 ± 1 °C). After 1.5 h of ischemia, the suture was removed, the thread plug was slowly pulled out for the purposes of ischemia-reperfusion, and the skin was sutured. In the sham operation group, the CCA, the ICA and the ECA were only separated and no thread plug was inserted. Based on the five-point scale used by Longa et al. [24], the rats were successfully divided into groups based on neurological deficit scores from 0 to 3. Rats that died within a few hours and those that had a thread plug that was deeply inserted under the subarachnoid hemorrhage were excluded.

Grouping and Administration

To confirm the effects of luteolin on I/R-induced rats, the animals were randomly divided into six groups (n = 15 for each group): (1) the sham group: in which the rats underwent the same surgical procedures as rats in the I/R group without filament insertion and received the vehicle; (2) the I/R group, in which the rats were subjected to 1.5 h of ischemia and injected with sodium hydrogen carbonate of the same volume; (3) the resveratrol group, in which 50 mg/kg of resveratrol [25] was gavaged. (4) the I/R + low-dose luteolin group, in which luteolin was injected intraperitoneally in rats at a dosage of 15 mg/kg after 1.5 h of ischemia; (5) the I/R + intermediate-dose luteolin group, in which luteolin (30 mg/kg) was injected intraperitoneally after 1.5 h of ischemia; (6) the I/R + high-dose luteolin group, in which luteolin (60 mg/kg) was injected intraperitoneally after 1.5 h of ischemia. The dose of luteolin used in this study is based on the study of luteolin on neuroprotection in a model of middle cerebral artery occlusion [26]. All experimental groups were dosed once a day for three consecutive days. In order to accurately reflect the proliferation of cells, we intraperitoneally injected 50 mg/kg of 5-bromo-2-deoxyuridine (BrdU, Sigma-Aldrich, USA) daily to rats 5 days before CIRI.

Measurement of Neurological Outcomes

After ischemia for 1.5 h and reperfusion for 3 days, neurological deficits were evaluated according to Longa et al. five-point scoring system. Briefly, rats with normal walking or with no neurological deficits scored 0; if the forepaws were

not fully extended and there were mild focal neurological deficits the score was 1; if there were contralateral rotation and moderate focal neurological deficits the score was 2; if deficits extended to the contralateral side or there were severe focal neurological deficits the score was three points. If the rat was immobile or had a low level of consciousness, the score was four points. The neurological deficit score was determined by a researcher who was blinded to the treatment the animal received. Zero and four points of animals were excluded, and one-three points of rats were included in the statistical standard. After modeling, 12 rats died, including one in the sham group, two in the I/R group , two in the resveratrol group, two in the I/R + low-dose luteolin group, three in the I/R + intermediate-dose luteolin group and two in the I/R + high-dose luteolin group. To ensure the same number of animals in each group, we filled the corresponding MCAO model in subsequent experiments. The data of 15 rats in each group were averaged and expressed by mean ± standard deviation, and compared with six groups.

Brain Tissue Preparation

After nerve function was measured, 15 rats in each group were anesthetized and sacrificed. All experimental animals were sacrificed and taken three days after administration. Five rats in each group were subjected to hematoxylin and eosin (HE) staining, immunofluorescence staining and apoptosis measurement. The rats were perfused with 4% paraformaldehyde and fixed at 4 °C for 24 h. Adjacent 10 μm coronal paraffin sections were collected at the ipsilateral thalamic level. Three rats were tested for cerebral edema, and three were tested for TTC. The hippocampus and cortex of four rats were frozen in liquid nitrogen and then stored at −80 °C for PCR and Western blot.

Measurement of Brain Edema

After CIRI, the rats were sacrificed, and the head was decapitated. The left brain tissue was isolated, weighed, and oven-dried until a constant weight was reached. The water content of the brain tissue was measured by the wet and dry weight method. The brain tissue water content was calculated as follows: brain tissue water content (%) = [(wet weight−dry weight)/wet weight] × 100%

Assessment of the Cerebral Infarct Size

2,3,5-Triphenyltetrazolium chloride (TTC, Lot: T8877; Sigma-Aldrich, USA) staining was performed to determine the cerebral infarct size. Rats in each group were randomly selected for TTC staining. After anesthesia, the olfactory bulb, frontal bone, cerebellum and lower brain stem were removed. The rats were immersed in normal saline and placed in a −20 °C refrigerator for 20 min. Coronal sections were removed, and the thickness of each slice was approximately 4 mm. A total of three slices were incubated in 2% TTC solution for 30 min (37 °C, without light) and soaked in 10% neutral formalin solution for 24 h. The analysis software Image Pro-Plus 6.0 was used to calculate the area of each cerebral infarction, which was multiplied by the thickness to obtain the infarct volume for each rat and calculate the percentage of the cerebral infarction volume [27].

The percentage of corrected infarct volume was calculated by using the following equation: percentage of corrected infarct volume = [contralateral hemisphere area−(ipsilateral hemisphere area measured infarct area contralateral hemisphere area)]/% × 100.

H&E Staining and Immunofluorescence Staining

The brain tissue was sectioned in paraffin and placed in a 65 °C oven for 30 min. Paraffin Section were dewaxed with xylene and placed in a gradient ethanol to hydrate. The tissues were placed in hematoxylin staining solution for 2 min, rinsed for 5 min in running water, differentiated, stained and dehydrated. Then, the neutral resin was sealed and ventilated, and the changes in neurons in the cortex and hippocampal CA1 area were observed under a microscope.

Paraffin sections were routinely dewaxed, washed three times with PBS, microwaved for repair three times, and washed with PBS three more times. The blocking solution was added and the sections were incubated at room temperature for 30 min, after which anti-BrdU (1:100 dilution), anti-DCX, anti-GFAP (1:1000 dilution; Abcam, Cambridge, UK), and anti-Iba-1 (1:1000 dilution; Abcam, Cambridge, UK) were added, and sections incubated overnight in a refrigerator at 4 °C. The wet box was removed from the refrigerator and rewarmed for 20 min, and sections were washed in PBS three times. FITC/TRITC fluorescent secondary antibody (mouse anti-rabbit, 1:200 [Santa Cruz Biotechnology, CA, USA] or rabbit anti-goat, 1:200 [Santa Cruz Biotechnology, CA, USA]; 50 μL/tablet) was added, and sections were incubated in the dark for 30 min and washed with PBS three times. DAPI was added to stain the nucleus, and sections were sealed and incubated at room temperature for 5 min and washed with PBS three times. Sections were then sealed and subject to laser scanning confocal microscopy. Then, Image-Pro Plus six image analysis software was used to the count BrdU+/DCX+ positive cells and the Iba-1/GFAP positive cells via laser scanning confocal microscopy.

The Degree of Mitochondrial Swelling, the Mitochondrial Membrane Potential, the Mitochondrial Reactive Oxygen Species (ROS) and the Manganese Superoxide Dismutase (SOD) Activity were Measured

The mitochondrial ROS, SOD activity and membrane potential were measured according to the instructions that were included with the kit (Jiancheng Bioengineering Institute, Nanjing, JS, China). The degree of mitochondrial swelling was determined by adding 200 μl of mitochondrial swelling response buffer and the proper amount of mitochondrial heavy suspension into a 96-well plate; the mitochondrial concentration was 0.25 μg/μl, and 1 μl of 0.05 M CaCl2 was added. After blending, the change in absorbance at 520 nm at 25 ℃ was recorded.

Apoptosis Experiment

The prepared paraffin sections were subjected to TUNEL staining to detect apoptosis in the brain tissue from each group. The method was carried out according to the instructions included with the TUNEL assay kit (Roche Molecular Biochemicals, Inc., Mannheim, Germany). Each paraffin section was incubated in a bead bath at 60 °C and treated with transparent xylene and an alcohol gradient. The section was then incubated with proteinase K at 37 °C for 30 min and washed with phosphate-buffered solution (PBS) three times, after which 50 μl of TUNEL reaction solution was added. DAPI dye solution was added to cover the tissue at room temperature for 15 min, and sections were rinsed three times and sealed with a water-soluble tablet. Five pathologies without random crossover were randomly selected from each pathological section and observed under a light microscope.

Detection of SIRT3, AMPK and mTOR RNA Expression in Brain Tissue via Real-Time Fluorescent Quantitative RT-PCR

The brain tissue of rats was obtained 3 days after MCAO, and the total RNA was extracted by using TRIzol reagent (Invitrogen, New York, USA). The quality of the total RNA was measured by UV spectrophotometry and agarose gel electrophoresis. cDNA was synthesized by using the PrimeScriptTM reverse transcription kit, and the reverse transcription product was diluted five times and used for subsequent real-time PCR analysis. Based on the mRNA sequences of rat SIRT3, AMPK, mTOR and β-actin published in the NCBI database, RT-PCR primers were designed using Oligo 6.0 software that would yield target fragments that spanned two exons. The primer sequences used were as follows: SIRT3-F: CCCGACTGCTCATCAA; SIRT3-R: CACCAG CCTTTCCACA; AMPK-F: TTGCCCAGTTACCTCTTT CC; AMPK-R: GGTTCATTATTCTCCGATTGTC; mTOR-F: TGGCATCGTGCTGTTGGGTG; mTOR-R: TCAAGT ATGGCAGGCGTGGG; ACTIN-F: TCCTGTGGCATC CATGAAACT; ACTIN-R: GAAGCATTTGCGGTGCAC GAT. All primers were synthesized by Shanghai Maxim Biological Co., Ltd. The following RT-PCR amplification conditions were used: predenaturation at 95℃ for 5 min, followed by 35 cycles of denaturation at 95℃ for 30 s, annealing at 60℃ for 30 s, and extension at 72℃ for 30 s. Using β-actin as an internal reference, the data were subjected to relative quantitative analysis using the 2-ΔΔCt method.

The difference in gene expression (2-ΔΔCt) was calculated using the equation 2-ΔΔCt = experimental group (target gene Ct value−internal reference gene Ct value)−control group (target gene Ct value−internal reference gene Ct value).

Western Blot Analysis of SIRT3, AMPK, p-AMPK, mTOR and p-mTOR Protein Expression in Brain Tissue

The remaining brain tissue was obtained, and the brain tissue homogenate was repeatedly milled at a low temperature. The appropriate amount of RIPA lysis buffer (Beyotime, Nanjing, Jiangsu, China) was added, and the supernatant was obtained after centrifugation at 4 °C. The total protein concentration was measured by BCA assay (Beyotime, Nanjing, Jiangsu, China) method. Twenty micrograms of whole protein lysate was loaded and subjected to 12% SDS-PAGE. After electrophoresis, the proteins were transferred to a nitrocellulose membrane. After blocking and rinsing, SIRT3 (Abcam, Cambridge, MA, USA; 1:100), AMPK (Santa Cruz, Dallas, Texas, USA; 1:1000), p-AMPK (Santa Cruz, Dallas, Texas, USA; 1:1000), mTOR (Santa Cruz, Dallas, Texas, USA; 1:1000) and p-mTOR (Santa Cruz, Dallas, Texas, USA; 1:1000) antibodies were added. The primary antibody (1:1000) was incubated in a refrigerator at 4 °C overnight, and then the horseradish peroxidase-labeled secondary antibody (1:2000) was added. The membrane was washed, developed via chemiluminescence, exposed and photographed. The acquired images were analyzed using Image-Pro Plus 6.0 image processing software, and the relative expression levels of the proteins were expressed as the ratio of the intensity of the SIRT3 and GAPDH protein bands.

Statistical Analysis

All values were expressed as the mean ± standard deviation. Statistical analysis was performed using SPSS 21.0 software (SPSS, Inc., Chicago, IL, USA). Statistical significance was calculated via one-way ANOVA with Dunnett's t-test as a

correction. $P < 0.05$ was considered to indicate a statistically significant difference.

Results

Luteolin can Alleviate Neurological Deficits in MCAO Rats

We studied the effect of luteolin on the symptoms of neurological dysfunction caused by cerebral ischemia. As shown in Fig. 1b, there were no signs of neurological deficit in the sham group. Compared with the sham group, the neurological scores at 24 h (4.58 ± 0.72), 48 h (4.12 ± 0.47), and 72 h (4.03 ± 0.62) were significantly increased in the model group, which indicated the presence of neurobehavioral disorder. Luteolin treatment effectively improved functional impairment at all tested times, and there was an overall difference between the model and luteolin groups ($p < 0.01$).

As shown in Fig. 1c and Table 1, the body weight of each group was measured 1 h before surgery, and the weights of the rats in the sham, model and drug groups were stable and showed no significant differences ($p > 0.05$). At 24, 48 and 72 h postsurgery, the body weights in the model group were significantly lower than in the sham group. The luteolin intermediate-dose and high-dose groupsand the resveratrol group showed significantly less reduction in body weight after CIRI ($p < 0.01$), which might be partially attributable to the improvement in neurobehavioral deficits.

Luteolin can Alleviate Brain Edema in MCAO Rats

The results showed that cerebral edema in the model group was significantly higher than in the sham-operated group ($p < 0.01$). After treatment, the degree of cerebral edema in groups treated with different doses of luteolin and the positive drug group was decreased ($p < 0.05$ and $p < 0.01$, respectively). Compared with the low-dose luteolin group, the degree of brain edema in the high- and intermediate-dose and positive drug groups was decreased ($p < 0.05$); the degree of edema in the intermediate-dose luteolin group was equivalent to that in the resveratrol group, and no statistically significant difference was found (Fig. 2c).

Luteolin can Reduce Cerebral Infarction Volume in MCAO Rats

The brain tissue sections obtained from the sham-operated group were all reddish in color after TTC staining, and no infarcts were found. Fig. 2a showed a typical photograph of coronal sections in sham, MCAO and luteolin-treated rats. The brain tissue staining in the model group and the luteolin low-dose group showed obvious white infarcts that were mainly located in the left frontal lobe, parietal cortex and striate. The volume ratios of the infarcts in the intermediate- and high-dose luteolin groups and the positive treatment group were significantly lower (20.69 ± 0.94%, 15.34 ± 0.82%, and 18.24 ± 0.93%, respectively) than that in the model group (49.65 ± 1.38) and the low-dose luteolin group (41.23 ± 2.32%; $p < 0.05$, Fig. 2b).

Luteolin can Reduce Morphological Changes in the Cortex and Hippocampus After Cerebral Infarction in MCAO Rats

To confirm the effect of luteolin on the number of neurons in the hippocampal CA1 region in rats, we observed the hippocampal CA1 region on the left side of the rat brain. In the sham group, the pyramidal neurons in the CA1 region had three-four layers after HE staining of the brain sections of rats. The tissue structure was normal, and the cells were arranged tightly and orderly; the endothelial cell structure integrity was intact, and the nucleolus was clear. In addition, the cytoplasm was stained evenly in the hippocampus, and the number of nerve cells was not reduced. In the I/R model group, the pyramidal neurons in the hippocampal CA1 region were loose and sparse, the cell structure was indistinct and the number of cells was obviously reduced; nuclear pyknosis was observed in most cell nuclei, and dyeing of the cells was increased. Vacuolar degeneration between the cells of the vertebral body was observed and was accompanied by proliferation of the glial cells, and the loss of nerve cells in the hippocampal CA1 area in the model group was significantly increased ($p < 0.01$). After administration, the loss of nerve cells in the hippocampal CA1 area of rats in the intermediate- and high-dose luteolin groups and the resveratrol group was gradually decreased ($p < 0.01$). In the hippocampal CA1 region, the pyramidal neurons remained

Table 1 Changes in body weight in rats after reperfusion

Group	Sham	I/R	Resveratrol	I/R+Luteolin L	I/R+Luteolin M	I/R+Luteolin H
0h	285.76 ± 12.43	280.87 ± 13.11	282.35 ± 13.31	283.95 ± 11.25	279.43 ± 10.14	284.12 ± 12.28
24h	287.45 ± 12.56	282.35 ± 13.31	285.45 ± 11.34	282.43 ± 12.31	280.34 ± 10.24	285.42 ± 12.35
48h	291.43 ± 12.98	262.43 ± 13.09	279.34 ± 12.35	278.39 ± 11.65	276.34 ± 9.46	281.23 ± 10.31
72h	295.35 ± 10.34	251.17 ± 14.83	280.31 ± 13.15	275.28 ± 11.19	270.35 ± 9.38	282.35 ± 10.23

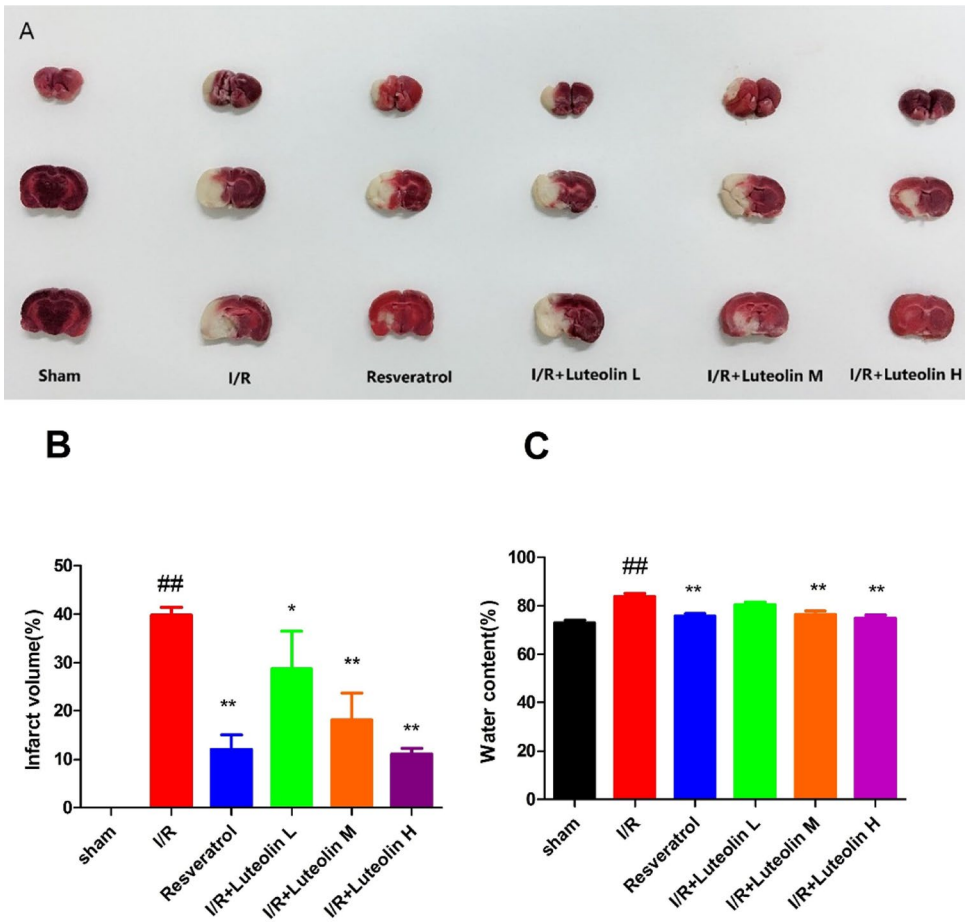

Fig. 2 Effects of luteolin on cerebral infarct area and water content in rats subjected to CIRI. **a** The area of cerebral infarction was measured by TTC staining, and the typical images of TTC staining were displayed after reperfusion. The red area represents normal brain tissue, and the pale area is the infarction and ischemic region. Luteolin reduced the cerebral infarct area in MCAO rats. **b** Evaluation of infarct area 72 h after reperfusion. After brain tissues were stained with TTC, the infarct area was evaluated using a morphological image analysis system. **c** The percentage of brain edema in each group was measured by the wet-dry method. Each bar represents the percentage of infarcts. The results are expressed as the mean ± SD. $^{\#\#}P < 0.01$, I/R vs the sham group; $^{*}P < 0.05$, $^{**}P < 0.01$, vs the I/R group.

normal and were arranged closely; the number of cells in the lamina of the vertebral body was increased, the nuclei were clear, and the capillary structure was relatively integrated. The degree of nerve cell survival was strikingly increased. Compared with the low-dose luteolin group, the number of pyramidal cells in the hippocampal CA1 area of rats in the intermediate- and high-dose luteolin groups was increased ($p < 0.05$; Fig. 3a and b).

HE staining showed that the neurons in the cortex of normal rat brains were arranged neatly and orderly and the nuclei were clear. In addition, the cell size was consistent and the cytoplasm was evenly colored; the fibers were consistent inF size and showed no evidence of degeneration or necrosis. In the model group, cells with necrotic foci of different sizes were observed. Numerous apoptotic cells around the necrotic foci. The nerve fibers in the brain tissue were disordered. The cells were swollen, the nucleoli had contracted and become necrotic, and the number of neurons was obviously reduced. After treatment with luteolin, the neuronal cell arrangement in rats treated with different doses and with positive drugs was slightly disordered. In the intermediate- and high-dose luteolin groups and the resveratrol group, the damage was slightly reduced and the degree of edema was decreased. In the high-dose luteolin group, the degree of neuronal cell damage was decreased, and the cell morphology had recovered; moreover, the cell membranes and nucleoli were intact, and some normal neuronal cells were seen. (Fig. 3c).

Luteolin can Alleviate Cell Apoptosis in MCAO Rats

The results showed that the cortical nerve cells of rats in the sham operation group were almost negative; the cells were evacuated and their structure was intact, and several positive cells were occasionally seen. Compared with the sham operation group, the number of positive apoptotic cells in the cortex of rats in the model group was significantly increased, and the difference was significant ($p < 0.01$). The rate of apoptosis in cells from rats treated with different doses of luteolin was significantly different from that found in the model group ($p < 0.01$), which indicated that different doses of luteolin can alleviate cell apoptosis in MCAO rats Intermediate and high doses were shown to significantly inhibit neuronal apoptosis in brain tissue, especially high doses (Fig. 4a and b).

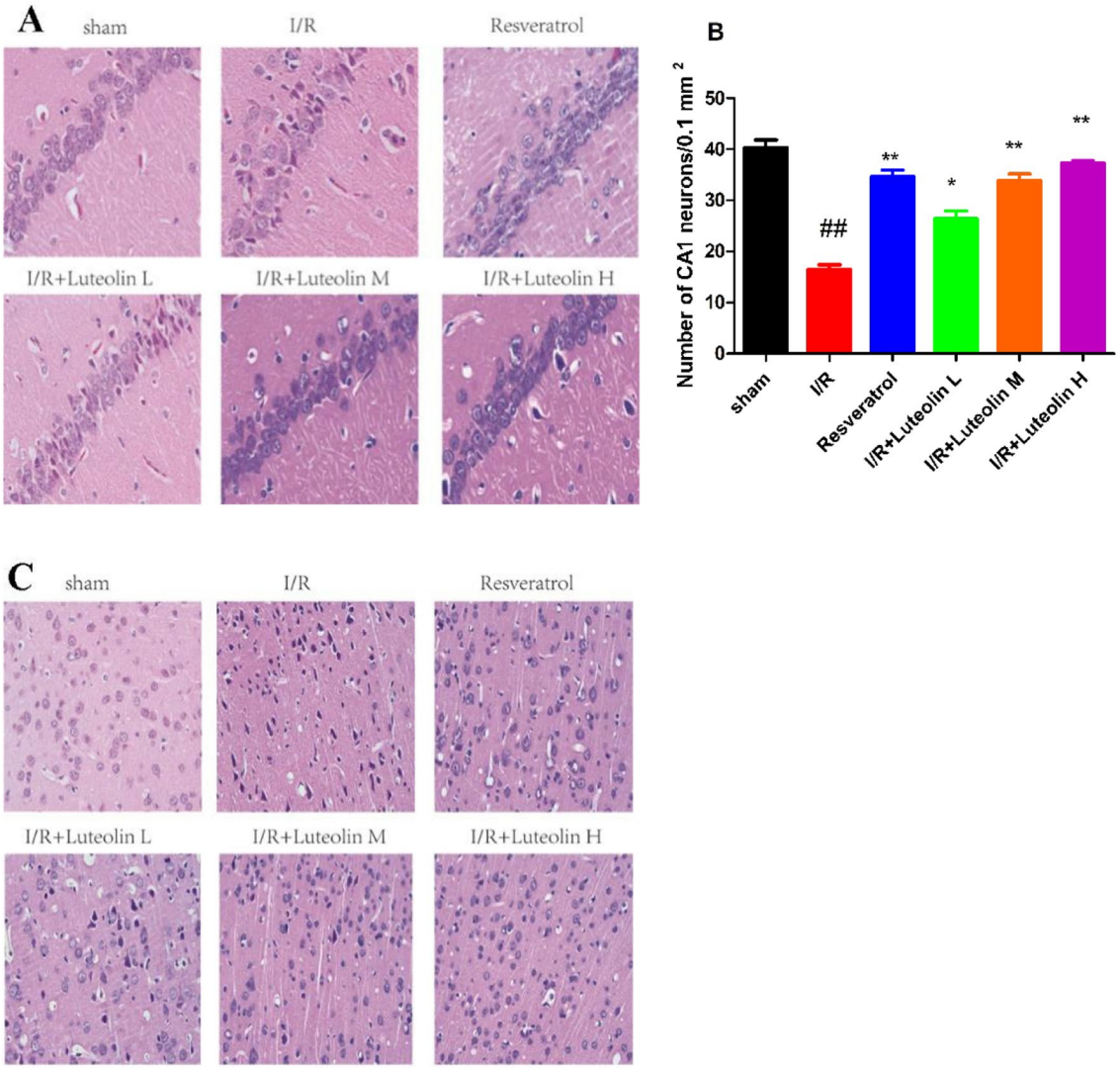

Fig. 3 Effects of luteolin on the histopathology of cortical and hippocampal CA1 neurons in rats subjected to ischemic reperfusion shown by HE staining. **a** Morphological changes in the hippocampal CA1 region were assessed by HE staining. **b** Nerve cell survival in the hippocampal CA1 region. **c** Pathological changes in the cerebral cortex in I/R rats (400× magnification). Values are expressed as the mean ± SD. $^{\#\#}P < 0.01$, I/R vs the sham group; $^{*}P < 0.05$, $^{**}P < 0.01$, vs the I/R group.

Luteolin can Reduce the Inflammatory Response in MCAO Rats

Activated astrocytes and invasive macrophages are closely associated with the development of postischemic neuroinflammation and neuronal damage. In the brain, GFAP is a well-known marker for astrocytes, and Iba-1 is specifically expressed in microglia. GFAP and Iba-1 have been identified as specific markers of astrocyte and microglia/macrophage activation, respectively. To evaluate the response to neuroinflammation after CIRI, we performed immunostaining for GFAP and Iba-1. As shown in Fig. 5a-d, almost all of the microglia obtained from rats in the sham group were at rest. Compared with the sham operation group, the number of GFAP- and Iba-1-positive cells in the hippocampus in rats in the model group was increased significantly, and Iba-1-positive microglia had been transformed mainly into activated cells; in addition, a large number of Iba-1- and GFAP-positive cells were observed in the hippocampus ($p < 0.01$). Compared with the model group, the average immunofluorescence intensity of GFAP- and Iba-1-positive cells in the hippocampus of rats after luteolin treatment was significantly reduced ($p < 0.01$). These results indicated that luteolin could inhibit the aggregation of microglia in the hippocampus within the ischemic area and the release of astrocytes and thereby exerted an anti-inflammatory effect.

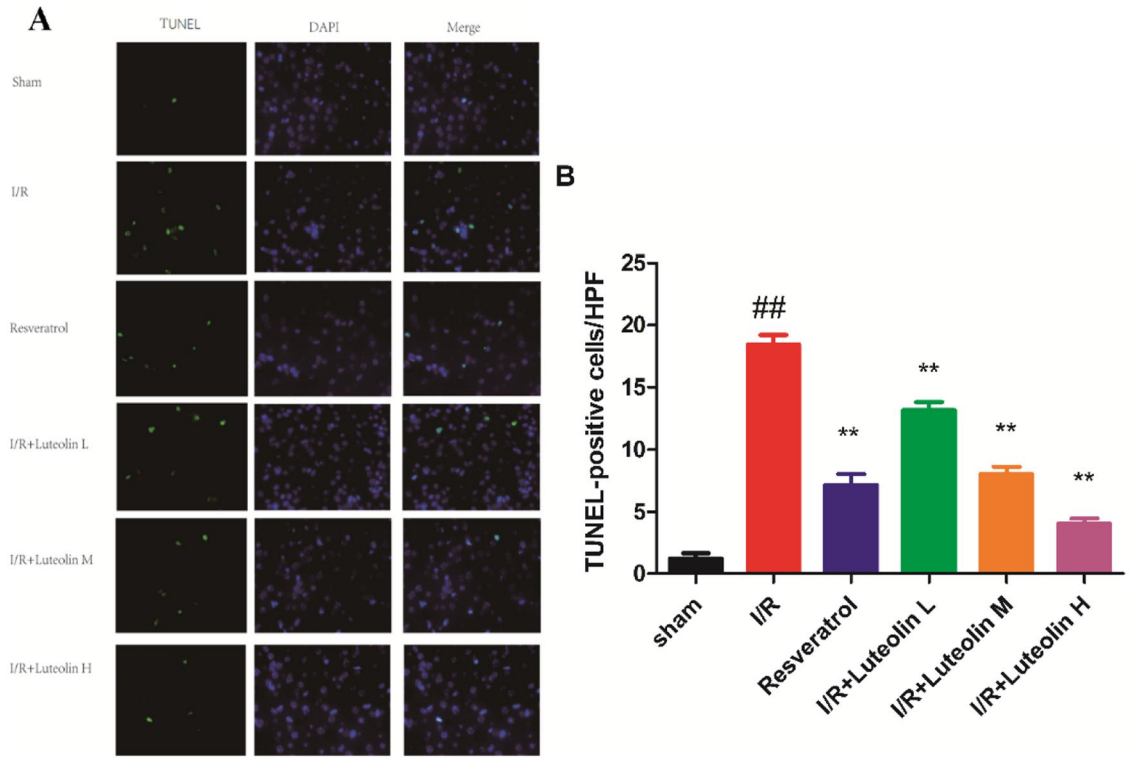

Fig. 4 Nuclei were stained with DAPI (blue); the TUNEL-positive cells served as a quantitative assessment of cell death (numbers per high-dose power field). **a** Changes in cerebral cortex cell apoptosis in I/R rats (400× magnification) **b** The number of TUNEL-positive cells resulting from cortex cell apoptosis. The results are expressed as the mean ± SD. $^{\#\#}P < 0.01$, I/R vs the sham group; $^{*}P < 0.05$, $^{**}P < 0.01$, vs the I/R group.

Luteolin Promotes Neurogenesis in MCAO Rats

The expression of BrdU+ cells in the DG of rats was detected by immunofluorescence, and proliferating cells in the DG region were labeled with BrdU. As shown in Fig. 6a, in the sham group, only a small number of BrdU+ cells were found in the DG area. In the model group, more BrdU+ cells were found in the DG area than in the sham group ($p < 0.01$). After treatment with different doses of luteolin and resveratrol, the number of BrdU+ cells were increased significantly in the hippocampal DG area ($p < 0.05$ and $p < 0.01$, respectively), especially in the high-dose luteolin group ($p < 0.01$). It was confirmed that luteolin can promote the proliferation of hippocampal DG cells in ischemic rats.

Immunofluorescence was used to detect the expression of DCX+ cells in the DG of rats. As shown in Fig. 6c, a small number of DCX+ cells were observed in the DG in the sham group and the model group. Compared with the sham group and the model group, the number of DCX+ cells in the DG in the intermediate- and high-dose luteolin groups and the positive drug groups was increased significantly ($p < 0.01$), especially in the high-dose luteolin group ($p < 0.01$).

Luteolin can Regulate the SIRT3/AMPK/mTOR Signing Pathway in MCAO Rats

To explore the mechanism underlying luteolin-induced protection against cerebral hypoperfusion, we further evaluated the effect of luteolin on the SIRT3/AMPK/mTOR pathway in brain tissue. We examined the expression of SIRT3, AMPK and mTOR mRNA using a semiquantitative RT-PCR assay. Furthermore, the expression of SIRT3, AMPK and mTOR in periinfarct zones of the ischemic cortex were examined. As shown in Fig. 7a-c, the level of AMPK mRNA in MCAO rats increased significantly, while the level of SIRT3 and mTOR mRNA decreased significantly ($p < 0.01$). After treatment with luteolin and resveratrol, the level of AMPK mRNA decreased and the levels of SIRT3 and mTOR mRNA increased significantly ($p < 0.05$ and $p < 0.01$, respectively). The effect of the intermediate- and high-dose luteolin groups and the resveratrol group was especially significant ($p < 0.01$).

Western blotting was carried out for each region, as shown in Fig. 7d. The results showed that after CIRI, the phosphorylation of AMPK increased and the expression of SIRT3 and mTOR protein decreased significantly ($p < 0.01$). After treatment with resveratrol and luteolin, the

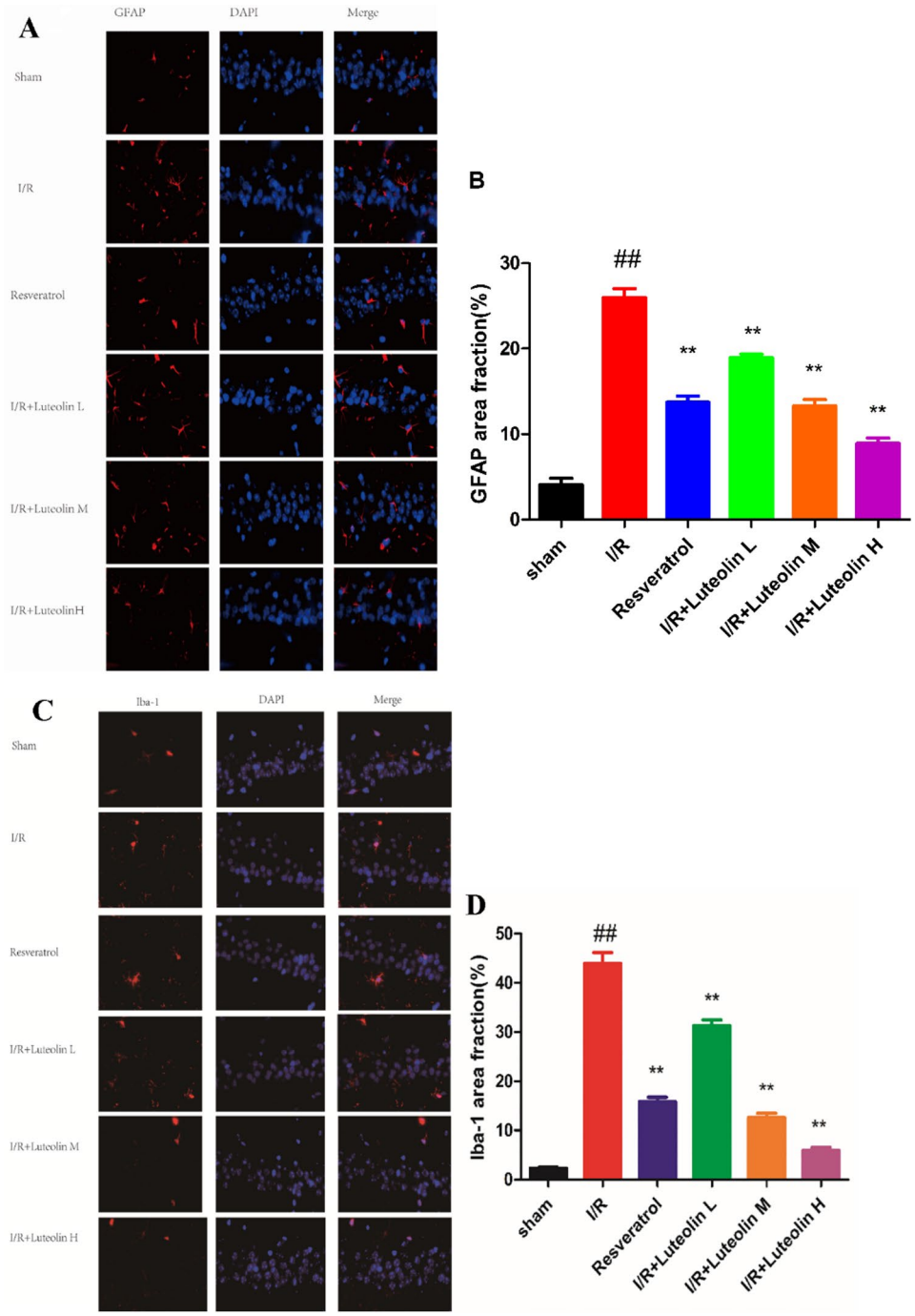

Fig. 5 Effects of luteolin on neuroinflammatory responses in ischemic brain tissue induced by CIRI. Immunofluorescent staining was performed 72 h after surgery. **a** Representative images of GFAP counterstained with DAPI in the CA1 subregion (400× magnification). **b** Quantitative image analysis of the immunoreactivity of GFAP based on the area fraction of GFAP-positive immunostaining in the CA1 area. **c** Representative images of Iba-1 immunostaining in the CA1 subregion (400x magnification). **d** Quantitative image analysis of Iba-1 immunoreactivity based on the area fraction of Iba-1 immunostaining in the CA1 area. The results are expressed as the mean ± SD. $^{\#\#}P < 0.01$, I/R vs the sham group; $^{**}P < 0.01$, vs the I/R group.

phosphorylation of AMPK decreased significantly, while the expression of the SIRT3 and mTOR proteins increased significantly ($p < 0.05$ and $p < 0.01$, respectively). In particular, a high dose of luteolin significantly inhibited the increase in AMPK phosphorylation and increased SIRT3 and mTOR expression in the brain after cerebral ischemia ($p < 0.01$). Therefore, these results suggested that the SIRT3/AMPK/mTOR signaling pathway might play a role in intracellular signaling that resulted in luteolin-induced nerve cell death suppression.

Changes in Mitochondrial Function after CIRI and the Effect of Luteolin

As shown in Fig. 8b-d, compared with the sham-operated group, the production of reactive oxygen species (ROS) in mitochondria increased, and the degree of swelling in mitochondria and the mitochondrial membrane potential decreased significantly in the model group ($p < 0.01$). After administration of luteolin and resveratrol, the production of mitochondrial reactive oxygen species decreased, and the

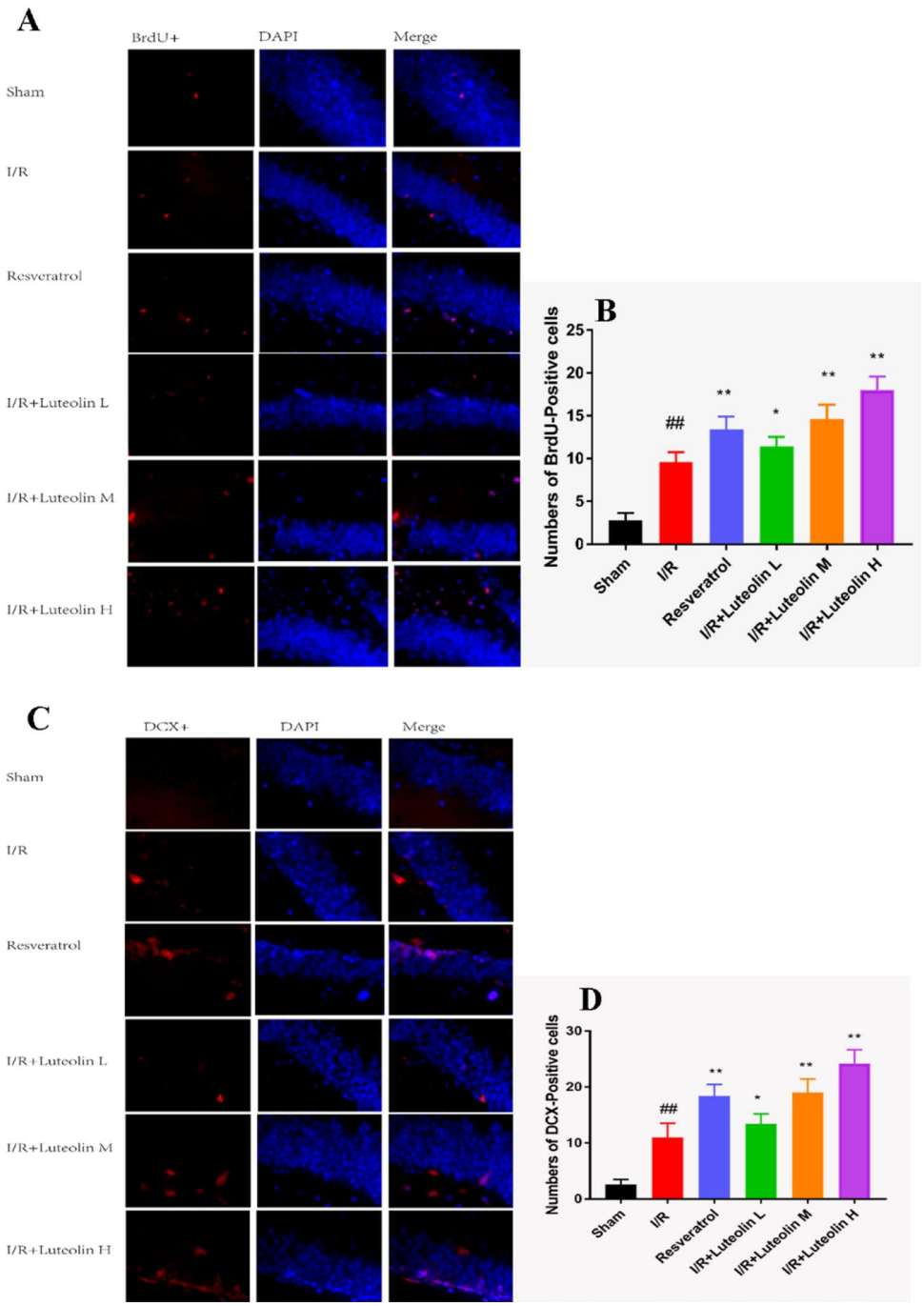

Fig. 6 Effects of luteolin on neurogenesis in ischemic brain tissue induced by CIRI in rats. Immunofluorescent staining was performed 72 h after surgery. **a** Representative images of BrdU+ cells in the DG subregion (400× magnification). **b** The number of BrdU+ cells in the DG in rats in each group. **c** Representative images of DCX+ cells in the DG subregion (400× magnification). **d** The number of DCX+ cells in the DG in rats in each group. The results are expressed as the mean ± SD. $^{\#\#}P < 0.01$, I/R vs the sham group; $^{*}P < 0.05$, $^{**}P < 0.01$, vs the I/R group.

degree of mitochondrial swelling and the mitochondrial membrane potential increased in model group rats ($p < 0.05$ and $p < 0.01$, respectively). Especially in the positive drug group and the luteolin intermediate- and high-dose groups, the curative effect was significant ($p < 0.01$). In addition, as shown in Fig. 8a, the activity of SOD in mitochondria decreased significantly in the model group, and luteolin increased the activity of SOD in mitochondria ($p < 0.05$). These results suggest that luteolin can significantly improve mitochondrial function after CIRI.

Discussion

SIRT3 maintains mitochondrial function, energy production, metabolism, apoptosis and intracellular signaling control. It has been shown that up-regulation of SIRT3 can activate the downstream signaling pathway AMPK/mTOR and has an improved neuroprotective effect in the treatment of ischemic cerebrovascular diseases [28]. It is generally believed that neuroprotective therapy is an effective strategy to reduce neuronal injury during cerebral ischemia-reperfusion, but

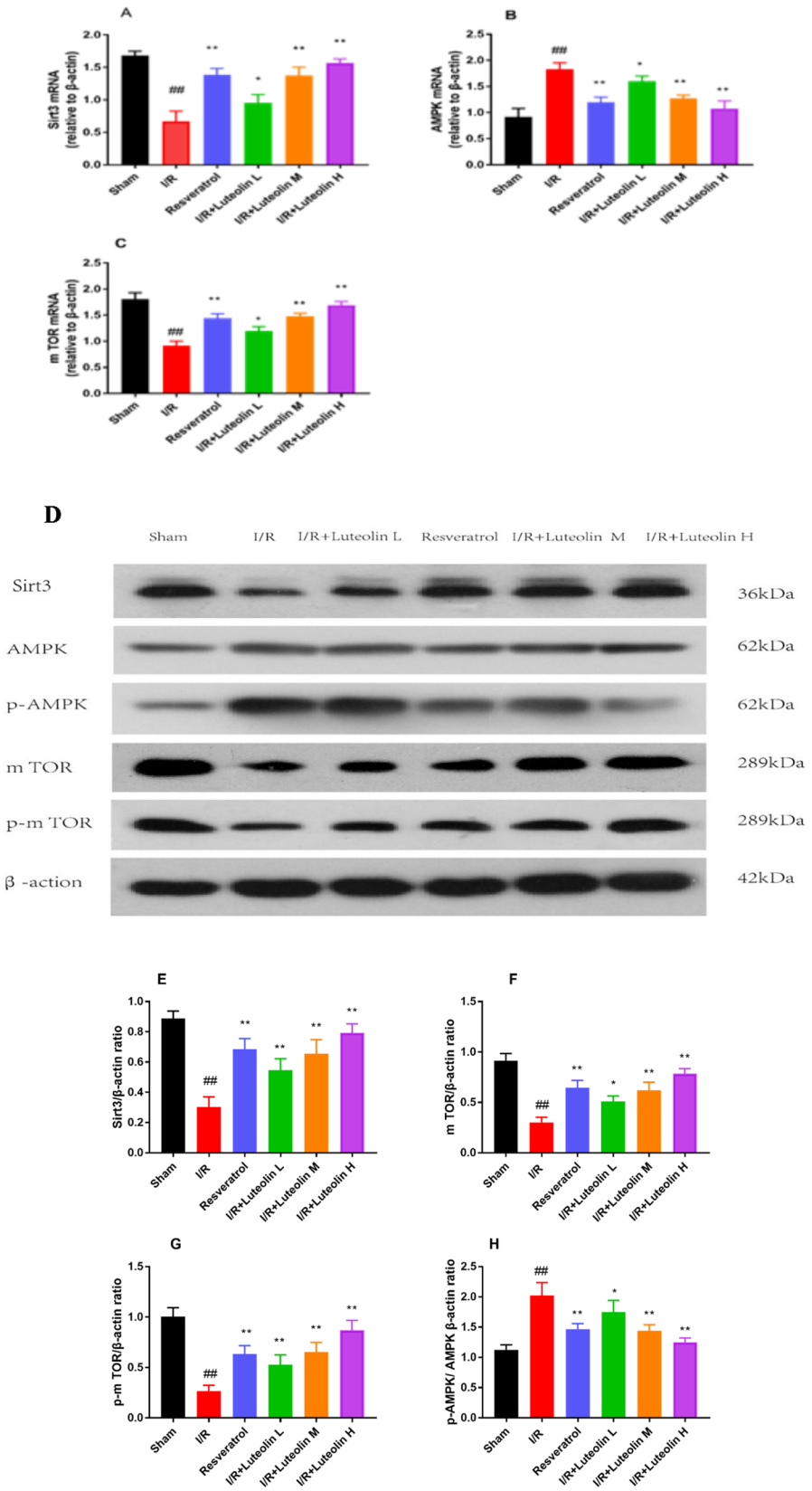

Fig. 7 Effects of luteolin on the regulation of the SIRT3/AMPK/mTOR signaling pathway in ischemic brain tissue induced by CIRI in rats. PCR and Western blot were performed 72 h after surgery. **a**–**c** Quantitative analysis of the mRNA expression of SIRT3, AMPK and mTOR as determined by RT-PCR. **d** Representative β-actin-normalized immunoblotting images and quantification of the key molecules SIRT3, AMPK and mTOR in hippocampal extracts from each group. **e**–**h** Protein levels of SIRT3, AMPK and mTOR in each group. The results are expressed as the mean ± SD. $^{\#\#}P < 0.01$, I/R vs the sham group; $^{*}P < 0.05$, $^{**}P < 0.01$, vs the I/R group.

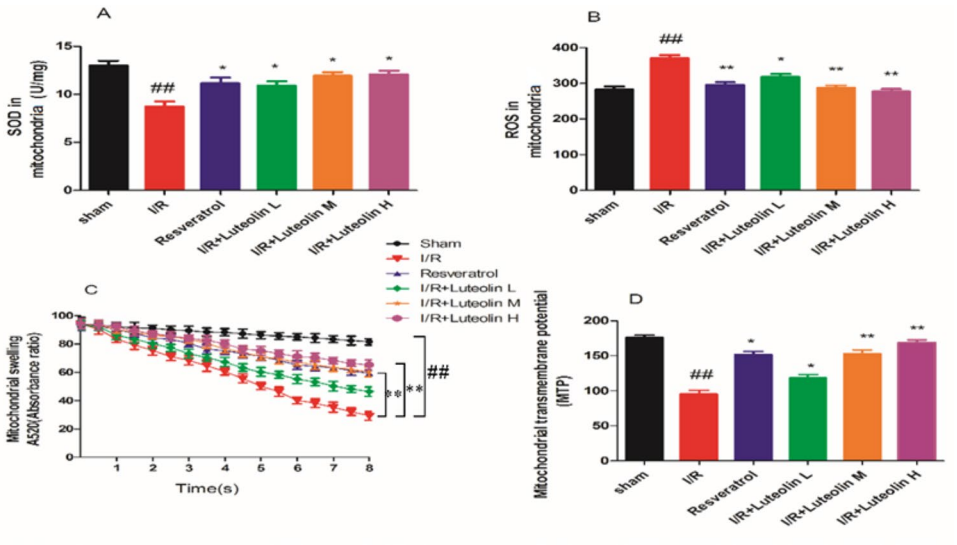

Fig. 8 Effects of luteolin on mitochondrial function in ischemic brain tissue induced by CIRI in rats. Based on the instructions in the kit, the assays were performed 72 h after surgery. **a** SOD in mitochondria **b** ROS in mitochondria. **c** Mitochondrial swelling at A520 (absorbance ratio). **d** Mitochondrial transmembrane potential. The results are expressed as the mean ± SD. $^{\#\#}P < 0.01$, I/R vs the sham group; $^{*}P < 0.05$, $^{**}P < 0.01$, vs the I/R group.

few effective drugs have been found during the experimental study of neuroprotective agents and their underlying mechanisms. Luteolin is a neuroprotective monomer used in Chinese medicine that plays a unique neuroprotective role in early brain injury resulting from CIRI due to its significant anti-inflammatory and antioxidant effects. A recent study showed that rats injected with luteolin (30 and 50 mg/kg) for 3 consecutive days showed reduced brain edema and neuronal apoptosis. Fu et al. recently reported that luteolin can protect against cognitive dysfunction induced by chronic cerebral hypoperfusion in rats [29]. Resveratrol (RES) is a recognized natural product for the treatment of cerebral ischemia. Many researchers have used it as a positive drug because of its remarkable effect. RES is a red wine-rich natural polyphenol with the ability to protect rats from cerebral ischemia/reperfusion injury [25]. Studies have shown that RSV treatment can alleviate oxidative stress, inhibit inflammation, and reduce lesion volume in animal traumatic brain injury models [30, 31]. Compared this as a positive drug with valeric acid to further verify the therapeutic effect of valeric acid. This study was designed to establish a rat model of focal cerebral ischemia-reperfusion. The results showed that intermediate and high doses of luteolin could significantly reduce the volume of ischemic brain injury and cerebral edema in rats, reduce the degree of neurological damage, improve the pathological and morphological changes in the cerebral cortex, increase the survival rate of CA1 region nerve cells, significantly inhibit the excessive activation of GFAP and Iba-1 in glial cells, inhibit cell apoptosis, and promote nerve cell regeneration. Its specific mechanism of action may be through the upregulation of SIRT3, which activates the AMPK/mTOR signaling pathway to exert neuroprotective effects. These results provide direct evidence that luteolin may be an exogenous neuroprotective agent that protects against damage caused by acute ischemic stroke.

To confirm whether luteolin treatment can reduce delayed neuronal death induced by CIRI, we evaluated the histopathological morphology of brain tissue. The results of HE staining show that there were a large number of apoptotic cells around the necrotic foci and that the nerve fibers in the brain tissue were disordered, and it was also observed that the cells were swollen and the nucleoli were contracted and necrotic. Nerve cell loss in the hippocampal CA1 area in rats from the model group was significantly increased (Fig.3). It was confirmed that CIRI could induce the death of neurons in the fragile CA1 area of the hippocampus. After treatment with luteolin, the neuronal cell arrangement was slightly disordered at different doses of luteolin and in the presence of positive drugs; TUNEL staining suggested that resveratrol and intermediate and high doses of luteolin can significantly inhibit neuronal apoptosis in brain tissue (Fig.4). These data proved that luteolin exerted a neuroprotective effect against pathological changes related to CIRI.

Ischemic injury can enhance neuronal responses and lead to the activation and proliferation of microglia [32]. Activated microglia can rapidly affect endogenous processes by modifying cell morphology and proliferation and the release of chemokines and cytokines and thus accelerate oligodendrocyte death, axonal degeneration and early BBB damage, which will eventually aggravate neuronal damage [33, 34]. Astrocytes, as the main cell population in the brain, are involved in many important signaling activities, including those involved in antioxidant activity, energy transfer, neurotransmitter uptake and recycling, ion homeostasis, trophic factor synthesis, and neurovascular coupling [35]. In pathological conditions, cerebral ischemia injury can activate astrocytes via a process known as reactive astrocytosis, which is characterized by cell hypertrophy and proliferation and increases in glial fibrillary acidic protein (GFAP). This activation also changes the expression of many other

molecules involved in cell structure, gene transcription, energy metabolism, intracellular signal transduction and membrane transport [36]. Therefore, regulating the activation of astrocytes and reducing the formation of glial scars can inhibit physical disturbance after brain injury and promote the regeneration of neurons. According to common morphological classification, Iba-1 cells are mainly divided into three types: resting cells, activated differentiated cells, and amoeba cells. Resting Iba-1 cells are characterized by small cell bodies and fine branching processes [37]. Our results showed that almost all microglial cells in the sham-operated group were at rest (Fig.5). Twenty-four hours after MCAO, the microglia cells had mainly transformed into activated cells, and a large number of deformed GFAP and Iba-1 cells were observed in the hippocampal area. After treatment, the average GFAP and Iba-1 fluorescence intensity in the luteolin groups and resveratrol group, especially the high-dose luteolin group, was significantly lower than that in the model group. These results suggest that luteolin limits the aggregation of microglia in the ischemic hippocampus area.

The study found that after the mammalian brain was fully developed, thousands of neurons were produced every day in the subgranular layer of the dentate gyrus of the hippocampus; although nerve regeneration almost completely stopped, immature neurons migrated from the subventricular zone (SVZ) to the olfactory bulb to produce crossover neurons [38]. The generation of new neurons in the dentate gyrus of the hippocampal region from neural precursor cells (NPC) resulted in the formation of excitatory granulosa cells and the main protruding neurons in the dentate gyrus region, which were derived from NPC [39]. These new neurons can be integrated into the neural loop to exert normal functioning. The results showed that neural regeneration in the hippocampus was closely related to memory functioning. Our results showed that there were a small number of BrdU+ and DCX+ cells in the dentate gyrus of rats in the sham group (Fig.6). Compared with the sham group, the BrdU+ and DCX+ cells in rats of the model group were gradually increased. Compared with the model group, the number of BrdU+ and DCX+ cells in the intermediate- and high-dose luteolin groups and the positive drug group were increased significantly, suggesting that luteolin can promote nerve regeneration and play a neuroprotective role. In addition, the release of inflammatory factors weakens the regenerative ability of adult nerves. The activation of microglia is directly related to the damage resulting from nerve regeneration [40]. After CIRI, the concentration of proinflammatory factors and the activation of microglia increased, resulting in leukocyte adhesion, aggregation and the release of several proinflammatory factors, such as IL-6, IL-10, and IFN-γ, which caused mitochondrial dysfunction and reactive oxygen species production [41]. Therefore, decreasing the activation of glial cells plays a crucial role in nerve regeneration after brain injury. On the one hand, when the brain is ischemic, the neurons in the brain are more susceptible to oxidative stress because they contain high concentrations of peroxidated unsaturated fatty acids; on the other hand, energy consumption is higher, and the level of antioxidative defense is lower [42]. There is increasing evidence that oxidative stress is one of the main causes of nerve damage caused by cerebral ischemia. Excessive production of reactive oxygen species not only leads to oxidative damage of proteins, lipids and nucleic acids but also leads to mitochondrial membrane permeation, resulting in cell death [43]. Our results showed that the activity of SOD in mitochondria decreased, the production of ROS in mitochondria increased, and the degree of swelling in mitochondria and the mitochondrial membrane potential decreased significantly in the model group. After administration of luteolin and resveratrol, the activity of SOD in mitochondria increased, mitochondrial ROS production decreased, and reversal of mitochondrial swelling and the mitochondrial membrane potential increased. Particularly in the positive drug group and the intermediate- and high-dose luteolin groups, the curative effect was significant, suggesting that luteolin may play a neuroprotective role by regulating oxidative stress and maintaining stable mitochondrial function.

SIRT3 can reduce mitochondrial DNA damage induced by ROS via deacetylation and stabilization of the DNA base excision repair enzyme OGG1 (8-oxoguanine-DNA glycosylase 1), which can repair mitochondrial DNA [44].Sestrins not only activate the antioxidant system in mitochondria but also induce the occurrence of mitochondrial autophagy [45]. It has been suggested that the key function of Sestrins is to regulate the activity of the AMPK/mTOR signaling pathway, and an increase in Sestrin can activate AMPK [46]. AMPK, as a serine threonine kinase, is a metabolic and stress-critical sensor and effector that is activated during nutritional deficiency, severe exercise or heat shock. Although the mechanism underlying the activation of AMPK by Sestrin is not clear, it has been reported that Sestrins can interact with AMPK and increase the amount of the AMPK subunit [47]. These results suggest that Sestrins may be involved in active regulation of the AMPK signaling pathway. LKB1 is the upstream activator of AMPK, and LKB1 is also a target of SIRT3 [48]. After SIRT3 deacetylation, activated LKB1 phosphorylates AMPK and activates it; phosphorylated AMPK can activate the TSC1-TSC2 complex to indirectly inhibit the mTOR protein complex to induce autophagy. In addition, AMPK can also directly inhibit the activity of the mTOR protein complex to induce autophagy [49]. However, the potential role of mTOR in a number of neurologic disorders so far are controversial. On the one hand, here is a growing body of evidence suggesting that rapamycin promotes neuronal viability and reduces neurological damage

in several ischemic injury models through inhibiting mTOR pathway [50, 51]. On the other hand, a large number of studies have shown that mTOR activation plays a protective role in ischemic brain injury [52, 53]. In a rat MCAO model, the activation of mTOR and its downstream target p70S6K by melatonin could prevent neuronal apoptosis and reduce infarct volume, while inhibition of mTOR activity by the mTOR inhibitor rapamycin could increase cerebral infarct volume. Through ischemic preconditioning and postischemic treatment, it was shown that the increased expression of mTOR in brain tissue after CIRI was beneficial in reducing infarct volume in cerebral tissue and improving deficiencies in behavior [54].

New research has shown that SIRT3 can improve insulin resistance through the AMPK signaling pathway [55]. In vitro, SIRT3 can activate PI3K/AKT signal transduction. The activation of SIRT3-induced AKT depends on AMPK, TSC2 and Rictor, which indicates that SIRT3 modulates AKT signaling via AMPK and mTORC2 [56]. These results suggest that SIRT3 plays an important role in regulating the activity of the AMPK/mTOR signaling pathway. Therefore, there is a positive feedback loop between processes involved in autophagy and SIRT3/AMPK. Based on previous research results, we believe that there is a positive feedback loop between SIRT3 and AMPK. Based on this, we can ascertain that SIRT3 activates the AMPK-mTOR signaling pathway and plays an important role in ischemic brain injury. Our results confirm that luteolin can ameliorate injury after CIRI at both the molecular and functional levels, and we explored the underlying mechanism. The results suggest that after CIRI, the phosphorylation of AMPK increased and the expression of SIRT3 and mTOR protein decreased significantly. After treatment with resveratrol and luteolin, the phosphorylation of AMPK decreased significantly, while the expression of the SIRT3 and mTOR proteins increased significantly (Fig.7). In particular, a high dose of luteolin could significantly inhibit the increase in AMPK phosphorylation and increase the expression of SIRT3 and mTOR in the brain after CIRI. Therefore, these results suggest that the SIRT3/AMPK/mTOR signaling pathway may play a role in intracellular signaling involved in luteolin-induced nerve cell death suppression.

Conclusion

In summary, luteolin can significantly improve neurological deficits in CIRI rats, improve pathological changes in the brain, inhibit apoptosis and inflammation, regulate oxidative stress, and promote hippocampal neurogenesis. Through in-depth research, we found that luteolin could upregulate hippocampal SIRT3 in rats suffering from cerebral ischemia, thus activating the downstream AMPK/mTOR signaling pathway and promoting the recovery of nerve function. Therefore, we believe that after treatment with luteolin, the AMPK/mTOR pathway is activated via the upregulation of SIRT3, which thereby inhibits the inflammatory reaction and apoptosis in rats after CIRI and promotes neurogenesis and the improvement of neurological deficits after ischemia. However, the mechanism underlying the specific interaction of luteolin with the SIRT3/AMPK/mTOR signaling pathway needs further investigation. Luteolin may have the potential to promote the treatment and recovery of cerebral ischemic patients in the clinic.

Funding This project is supported by the Jilin Province Development and Reform Commission Fund 2019C050-3

Compliance with Ethical Standards

Conflicts of interest The authors declare that they have no conflicts of interest.

References

1. Zhang Y, Wang Y, Xu J, Tian F, Hu S, Chen Y, Fu Z (2019) Melatonin attenuates myocardial ischemia-reperfusion injury via improving mitochondrial fusion/mitophagy and activating the AMPK-OPA1 signaling pathways. J Pineal Res 66:e12542
2. Hu J, Pang WS, Han J, Zhang K, Zhang JZ, Chen LD (2018) Gualou Guizhi decoction reverses brain damage with cerebral ischemic stroke, multi-component directed multi-target to screen calcium-overload inhibitors using combination of molecular docking and protein-protein docking. J Enzyme Inhibit Med Chem 33:115–125
3. Liu F, Lu J, Manaenko A, Tang J, Hu Q (2018) Mitochondria in ischemic stroke: new insight and implications. Ag Dis 9:924–937
4. Wei H, Li Y, Han S, Liu S, Zhang N, Zhao L, Li S, Li J (2016) cPKCgamma-modulated autophagy in neurons alleviates ischemic injury in brain of mice with ischemic stroke through Akt-mTOR pathway. Translat Stroke Res 7:497–511
5. Huang JL, Manaenko A, Ye ZH, Sun XJ, Hu Q (2016) Hypoxia therapy–a new hope for the treatment of mitochondrial dysfunctions. Med Gas Res 6:174–176
6. Amigo I, da Cunha FM, Forni MF, Garcia-Neto W, Kakimoto PA, Luevano-Martinez LA, Macedo F, Menezes-Filho SL, Peloggia J, Kowaltowski AJ (2016) Mitochondrial form, function and signalling in aging. Biochem J 473:3421–3449
7. Kim SC, Sprung R, Chen Y, Xu Y, Ball H, Pei J, Cheng T, Kho Y, Xiao H, Xiao L, Grishin NV, White M, Yang XJ, Zhao Y (2006) Substrate and functional diversity of lysine acetylation revealed by a proteomics survey. Mol cell 23:607–618
8. Wang XQ, Shao Y, Ma CY, Chen W, Sun L, Liu W, Zhang DY, Fu BC, Liu KY, Jia ZB, Xie BD, Jiang SL, Li RK, Tian H (2014) Decreased SIRT3 in aged human mesenchymal stromal/stem cells increases cellular susceptibility to oxidative stress. J Cell Mol Med 18:2298–2310
9. Finley LW, Haas W, Desquiret-Dumas V, Wallace DC, Procaccio V, Gygi SP, Haigis MC (2011) Succinate dehydrogenase is a direct target of sirtuin 3 deacetylase activity. PloS one 6:e23295

10. Osborne B, Cooney GJ, Turner N (2014) Are sirtuin deacylase enzymes important modulators of mitochondrial energy metabolism? Biochimica et biophysica acta 1840:1295–1302
11. Fu J, Jin J, Cichewicz RH, Hageman SA, Ellis TK, Xiang L, Peng Q, Jiang M, Arbez N, Hotaling K, Ross CA, Duan W (2012) trans-(-)-epsilon-Viniferin increases mitochondrial sirtuin 3 (SIRT3), activates AMP-activated protein kinase (AMPK), and protects cells in models of Huntington Disease. J Biol Chem 87:24460–24472
12. Pillai VB, Sundaresan NR, Kim G, Gupta M, Rajamohan SB, Pillai JB, Samant S, Ravindra PV, Isbatan A, Gupta MP (2010) Exogenous NAD blocks cardiac hypertrophic response via activation of the SIRT3-LKB1-AMP-activated kinase pathway. J Biol Chem 285:3133–3144
13. Dai SH, Chen T, Li X, Yue KY, Luo P, Yang LK, Zhu J, Wang YH, Fei Z, Jiang XF (2017) Sirt3 confers protection against neuronal ischemia by inducing autophagy: Involvement of the AMPK-mTOR pathway. Free Radical Biol Med 108:345–353
14. Lai YC, Tabima DM, Dube JJ, Hughan KS, Vanderpool RR, Goncharov DA, St Croix CM, Garcia-Ocana A, Goncharova EA, Tofovic SP, Mora AL, Gladwin MT (2016) SIRT3-AMP-activated protein kinase activation by nitrite and metformin improves hyperglycemia and normalizes pulmonary hypertension associated with heart failure with preserved ejection fraction. Circulation 133:717–731
15. Morrison A, Chen L, Wang J, Zhang M, Yang H, Ma Y, Budanov A, Lee JH, Karin M, Li J (2015) Sestrin2 promotes LKB1-mediated AMPK activation in the ischemic heart. FASEB J 29:408–417
16. Sanli T, Linher-Melville K, Tsakiridis T, Singh G (2012) Sestrin2 modulates AMPK subunit expression and its response to ionizing radiation in breast cancer cells. PloS one 7:e32035
17. Lopez-Lazaro M (2009) Distribution and biological activities of the flavonoid luteolin. Mini Rev Med Chem 9:31–59
18. Hytti M, Piippo N, Korhonen E, Honkakoski P, Kaarniranta K, Kauppinen A (2015) Fisetin and luteolin protect human retinal pigment epithelial cells from oxidative stress-induced cell death and regulate inflammation. Sci Rep 5:17645
19. Lin TY, Lu CW, Wang SJ (2016) Luteolin protects the hippocampus against neuron impairments induced by kainic acid in rats. Neurotoxicology 55:48–57
20. Qiao H, Dong L, Zhang X, Zhu C, Zhang X, Wang L, Liu Z, Chen L, Xing Y, Wang C, Li Y (2012) Protective effect of luteolin in experimental ischemic stroke: upregulated SOD1, CAT, Bcl-2 and claudin-5, down-regulated MDA and Bax expression. Neurochem Res 37:2014–2024
21. Siracusa R, Paterniti I, Impellizzeri D, Cordaro M, Crupi R, Navarra M, Cuzzocrea S, Esposito E (2015) The association of palmitoylethanolamide with luteolin decreases neuroinflammation and stimulates autophagy in Parkinson's disease model. CNS Neurol Disorders Drug Targets 14:1350–1365
22. Kwon Y (2017) Luteolin as a potential preventive and therapeutic candidate for Alzheimer's disease. Exp Gerontol 95:39–43
23. Tambe R, Patil A, Jain P, Sancheti J, Somani G, Sathaye S (2017) Assessment of luteolin isolated from Eclipta alba leaves in animal models of epilepsy. Pharmaceut Biol 55:264–268
24. Longa EZ, Weinstein PR, Carlson S, Cummins R (1989) Reversible middle cerebral artery occlusion without craniectomy in rats. Stroke 20:84–91
25. Liu Y, Yang H, Jia G, Li L, Chen H, Bi J, Wang C (2018) The Synergistic neuroprotective effects of combined rosuvastatin and resveratrol pretreatment against cerebral ischemia/reperfusion injury. J Stroke Cerebrovasc Dis 27:1697–1704
26. Xu J, Wang H, Ding K, Zhang L, Wang C, Li T, Wei W, Lu X (2014) Luteolin provides neuroprotection in models of traumatic brain injury via the Nrf2-ARE pathway. Free Radical Biol Med 71:186–195
27. Sun J, Tong L, Luan Q, Deng J, Li Y, Li Z, Dong H, Xiong L (2012) Protective effect of delayed remote limb ischemic postconditioning: role of mitochondrial K(ATP) channels in a rat model of focal cerebral ischemic reperfusion injury. J Cerebral Blood Flow Metabol 32:851–859
28. Zhang M, Deng YN, Zhang JY, Liu J, Li YB, Su H, Qu QM (2018) SIRT3 protects rotenone-induced injury in SH-SY5Y cells by promoting autophagy through the LKB1-AMPK-mTOR pathway. Ag Dis 9:273–286
29. Fu X, Zhang J, Guo L, Xu Y, Sun L, Wang S, Feng Y, Gou L, Zhang L, Liu Y (2014) Protective role of luteolin against cognitive dysfunction induced by chronic cerebral hypoperfusion in rats. Pharmacol Biochem Behav 126:122–130
30. Singleton RH, Yan HQ, Fellows-Mayle W, Dixon CE (2010) Resveratrol attenuates behavioral impairments and reduces cortical and hippocampal loss in a rat controlled cortical impact model of traumatic brain injury. J Neurotrauma 27:1091–1099
31. Lopez MS, Dempsey RJ, Vemuganti R (2015) Resveratrol neuroprotection in stroke and traumatic CNS injury. Neurochem Int 89:75–82
32. Kim DH, Yoon BH, Jung WY, Kim JM, Park SJ, Park DH, Huh Y, Park C, Cheong JH, Lee KT, Shin CY, Ryu JH (2010) Sinapic acid attenuates kainic acid-induced hippocampal neuronal damage in mice. Neuropharmacology 59:20–30
33. Zhang Q, Zhang J, Yan Y, Zhang P, Zhang W, Xia R (2017) Proinflammatory cytokines correlate with early exercise attenuating anxiety-like behavior after cerebral ischemia. Brain Behav 7:e00854
34. Wang Y, Huang Y, Xu Y, Ruan W, Wang H, Zhang Y, Saavedra JM, Zhang L, Huang Z, Pang T (2018) A dual AMPK/Nrf2 activator reduces brain inflammation after stroke by enhancing microglia M2 polarization. Antioxidants Redox Signal 28:141–163
35. Qiu Y, Pan J, Li Y, Li X, Li M, Abukhousa I, Wang Y (2011) Relationship between activated astrocytes and hypoxic cerebral tissue in a rat model of cerebral ischemia/reperfusion. Int J Neurosci 121:1–7
36. Liu Z, Chopp M (2016) Astrocytes, therapeutic targets for neuroprotection and neurorestoration in ischemic stroke. Progress Neurobiol 144:103–120
37. Ma Y, Wang J, Wang Y, Yang GY (2017) The biphasic function of microglia in ischemic stroke. Progress Neurobiol 157:247–272
38. Aimone JB, Deng W, Gage FH (2010) Adult neurogenesis: integrating theories and separating functions. Trends Cognit Sci 14:325–337
39. Volobouева LA, Giffard RG (2011) Inflammation, mitochondria, and the inhibition of adult neurogenesis. J Neurosci Res 89:1989–1996
40. Rola R, Raber J, Rizk A, Otsuka S, VandenBerg SR, Morhardt DR, Fike JR (2004) Radiation-induced impairment of hippocampal neurogenesis is associated with cognitive deficits in young mice. Exp Neurol 188:316–330
41. Esenwa CC, Elkind MS (2016) Inflammatory risk factors, biomarkers and associated therapy in ischaemic stroke. Nat Rev Neurol 12:594–604
42. Wilson AA, Sadovski O, Nobrega JN, Raymond RJ, Bambico FR, Nashed MG, Garcia A, Bloomfield PM, Houle S, Mizrahi R, Tong J (2017) Evaluation of a novel radiotracer for positron emission tomography imaging of reactive oxygen species in the central nervous system. Nuclear Med Biol 53:14–20
43. Andrabi SS, Parvez S, Tabassum H (2017) Progesterone induces neuroprotection following reperfusion-promoted mitochondrial dysfunction after focal cerebral ischemia in rats. Dis Models Mech 10:787–796

44. Cheng Y, Ren X, Gowda AS, Shan Y, Zhang L, Yuan YS, Patel R, Wu H, Huber-Keener K, Yang JW, Liu D, Spratt TE, Yang JM (2013) Interaction of Sirt3 with OGG1 contributes to repair of mitochondrial DNA and protects from apoptotic cell death under oxidative stress. Cell Death Dis 4:e731
45. Rhee SG, Bae SH (2015) The antioxidant function of sestrins is mediated by promotion of autophagic degradation of Keap1 and Nrf2 activation and by inhibition of mTORC1. Free Radical Biol Med 88:205–211
46. Zhao W, Zhang L, Chen R, Lu H, Sui M, Zhu Y, Zeng L (2018) SIRT3 protects against acute kidney injury via AMPK/mTOR-Regulated autophagy. Front Physiol 9:1526
47. Deng W, Cha J, Yuan J, Haraguchi H, Bartos A, Leishman E, Viollet B, Bradshaw HB, Hirota Y, Dey SK (2016) p53 coordinates decidual sestrin 2/AMPK/mTORC1 signaling to govern parturition timing. J Clin Invest 126:2941–2954
48. Li N, Huang D, Lu N, Luo L (2015) Role of the LKB1/AMPK pathway in tumor invasion and metastasis of cancer cells (Review). Oncol Rep 34:2821–2826
49. Dunlop EA, Tee AR (2013) The kinase triad, AMPK, mTORC1 and ULK1, maintains energy and nutrient homoeostasis. Biochem Soc Trans 41:939–943
50. Yin L, Ye S, Chen Z, Zeng Y (2012) Rapamycin preconditioning attenuates transient focal cerebral ischemia/reperfusion injury in mice. Int J Neurosci 122:748–756
51. Fletcher L, Evans TM, Watts LT, Jimenez DF, Digicaylioglu M (2013) Rapamycin treatment improves neuron viability in an in vitro model of stroke. PloS one 8:e68281
52. Yang GS, Zhou XY, An XF, Liu XJ, Zhang YJ, Yu D (2018) mTOR is involved in stroke-induced seizures and the anti-seizure effect of mild hypothermia. Mol Med Rep 17:5821–5829
53. Xie R, Wang P, Ji X, Zhao H (2013) Ischemic post-conditioning facilitates brain recovery after stroke by promoting Akt/mTOR activity in nude rats. J Neurochem 127:723–732
54. Liu P, Yang X, Hei C, Meli Y, Niu J, Sun T, Li PA (2016) Rapamycin reduced ischemic brain damage in diabetic animals is associated with suppressions of mTOR and ERK1/2 signaling. Int J Biol Sci 12:1032–1040
55. Li H, Liu S, Yuan H, Niu Y, Fu L (2017) Sestrin 2 induces autophagy and attenuates insulin resistance by regulating AMPK signaling in C2C12 myotubes. Exp Cell Res 354:18–24
56. Um SH, Frigerio F, Watanabe M, Picard F, Joaquin M, Sticker M, Fumagalli S, Allegrini PR, Kozma SC, Auwerx J, Thomas G (2004) Absence of S6K1 protects against age- and diet-induced obesity while enhancing insulin sensitivity. Nature 431:200–205